



## Stabilizing spin coherence through environmental entanglement in strongly dissipative quantum systems

Soumya Bera,<sup>1</sup> Serge Florens,<sup>1</sup> Harold U. Baranger,<sup>2</sup> Nicolas Roch,<sup>3,1</sup> Ahsan Nazir,<sup>4,5</sup> and Alex W. Chin<sup>6</sup>

<sup>1</sup>*Institut Néel, CNRS and Université Grenoble Alpes, F-38042 Grenoble, France*

<sup>2</sup>*Department of Physics, Duke University, Durham, North Carolina 27708, USA*

<sup>3</sup>*Laboratoire Pierre Aigrain, École Normale Supérieure, CNRS (UMR 8551), Université Pierre et Marie Curie, Université Denis Diderot, 24 rue Lhomond, 75231 Paris Cedex 05, France*

<sup>4</sup>*Blackett Laboratory, Imperial College London, London SW7 2AZ, United Kingdom*

<sup>5</sup>*Photon Science Institute, The University of Manchester, Oxford Road, Manchester M13 9PL, United Kingdom*

<sup>6</sup>*Theory of Condensed Matter Group, University of Cambridge, J J Thomson Avenue, Cambridge CB3 0HE, United Kingdom*

(Received 20 July 2013; revised manuscript received 26 February 2014; published 18 March 2014)

The key feature of a quantum spin coupled to a harmonic bath—a model dissipative quantum system—is competition between oscillator potential energy and spin tunneling rate. We show that these opposing tendencies cause environmental entanglement through superpositions of adiabatic and antiadiabatic oscillator states, which then stabilizes the spin coherence against strong dissipation. This insight motivates a fast-converging variational coherent-state expansion for the many-body ground state of the spin-boson model, which we substantiate via numerical quantum tomography.

DOI: [10.1103/PhysRevB.89.121108](https://doi.org/10.1103/PhysRevB.89.121108)

PACS number(s): 03.65.Yz, 03.65.Ud, 71.27.+a, 71.38.–k

The coupling of a quantum object to a macroscopic reservoir plays a fundamental role in understanding the complex transition from the quantum to the classical world. The study of such dissipative quantum phenomena has deep implications across a broad range of topics in physics [1], quantum technology [2], chemistry [3], and biology [4]. While quantum information stored in the quantum subsystem alone is lost during the interaction with the unobserved degrees of freedom in the reservoir, it is in principle preserved in the entangled many-body state of the global system. The nature of this complete wave function has received little attention, especially regarding the entanglement generated among the reservoir states. However, ultrafast experiments on solid-state and molecular nanostructures, including biological complexes, are increasingly able to probe the details of environmental degrees of freedom, whose quantum properties—particularly in nonperturbative regimes—may be key to understanding the device characteristics [5]. Our purpose here is to unveil a simple emerging structure of the wave functions in open quantum systems, using the complementary combination of numerical many-body quantum tomography and a systematic coherent-state expansion that efficiently encodes the entanglement structure of the bath. This combination of advanced techniques reveals how nonclassical properties of the macroscopic environment can stabilize quantum coherence with respect to a purely semiclassical response of the bath.

An archetype for exploring the quantum dissipation problem [6–8] is to start with the simplest quantum object, a two-level system describing a generic quantum bit embodied by spin states  $\{|\uparrow\rangle, |\downarrow\rangle\}$ , and to couple it to an environment consisting of an infinite collection of quantum oscillators  $a_k^\dagger$  (with continuous quantum number  $k$  and energy  $\hbar\omega_k$ ). Quantum superposition of the two qubit-states is achieved through a splitting  $\Delta$  acting on the transverse spin component, while dissipation (energy exchange with the bosonic environment) and decoherence are provided by a longitudinal interaction term  $g_k$  with each displacement field in the bath. This leads

to the Hamiltonian of the celebrated continuum spin-boson model (SBM) [6,7]:

$$H = \frac{\Delta}{2} \sigma_x - \sigma_z \sum_k \frac{g_k}{2} (a_k^\dagger + a_k) + \sum_k \omega_k a_k^\dagger a_k, \quad (1)$$

where we set  $\hbar = 1$ , and the sums can be considered as integrals by introducing the spectral function of the environment,  $J(\omega) \equiv \sum_k g_k^2 \delta(\omega - \omega_k)$ . The generality of the SBM makes it a key model for studying nonequilibrium dynamics, non-Markovian quantum evolution, biological energy transport, and the preparation and control of exotic quantum states in a diverse array of systems [3,6–9].

The possibility of maintaining robust spin superpositions in the ground and steady states of the SBM has attracted considerable attention, primarily due to its implications for quantum computing [10,11]. Previous numerical approaches have focused on observables related to the qubit degrees of freedom [12–19], while a description of the global system-environment wave function has been confined to variational studies [20–24]. Variational theory readily predicts the formation of semiclassical polaron states, which involve the adiabatic response of the environmental modes to the spin tunneling, and thus the generation of strong entanglement between the qubit and the bath. However, we shall demonstrate here that the ground state of Hamiltonian (1) contains additional nonclassical correlations among the environmental oscillator modes arising from their *nonadiabatic* response to spin-flip processes. We find that this entanglement structure is key for the stabilization of qubit superpositions relative to the semiclassical picture, and, in addition, follows naturally from a systematic variational framework beyond the adiabatic polaron approximation.

To reveal the nature of these emergent nonclassical environmental states, we start by analyzing the SBM with qualitative arguments based on energetics. First, in the absence of tunneling,  $\Delta = 0$ , the ground state of  $H$  in Eq. (1) is doubly degenerate. In the corresponding wave functions, the

oscillators displace classically, in a direction that is fully correlated with the spin projection (adiabatic response):  $|\Psi_{\uparrow}\rangle = |\uparrow\rangle \otimes |f^{\text{cl}}\rangle$  and  $|\Psi_{\downarrow}\rangle = |\downarrow\rangle \otimes |-f^{\text{cl}}\rangle$ . Here we introduce the product of semiclassical coherent states (displaced oscillators)  $|\pm f\rangle \equiv e^{\pm \sum_k f_k (a_k^\dagger - a_k)} |0\rangle$ , with the classical displacements  $f_k^{\text{cl}} = \pm g_k / 2\omega_k$  that shift each oscillator to the minimum of its static spin-dependent potential. This potential is evident in Eq. (1) for  $\Delta = 0$  and is shown explicitly in Fig. 1(a).

For  $\Delta \neq 0$ , the oscillators experience a competition between spin tunneling and oscillator displacement energy. For high-frequency modes ( $\omega_k \gg \Delta$ ), transitions to other oscillator states are suppressed by the steep curvature of the potential [Fig. 1(a)]. Thus, these oscillators adiabatically tunnel with the spin between potential minima; the displacement of the oscillators reduces their overlap, suppressing the tunneling amplitude to a value  $\Delta_R \ll \Delta$ . Extending this argument to low-frequency modes ( $\omega_k \ll \Delta$ ) reveals a problem: the large separation of the minima ( $g_k / 2\omega_k$ ) causes poor wave-function overlap that prevents tunneling of the spin, thus destroying spin superposition. The classic scenario to overcome this problem is to adjust the displacements to smaller values, sacrificing potential energy to maintain spin-tunneling energy through better overlap [Fig. 1(b)]. Here, we argue for an alternative scenario: because the potential surface is shallow for low-frequency modes, transitions to other oscillator states become possible. Indeed, it is favorable for the oscillator wave function to include superpositions of coherent states with displacements *opposite* to those dictated by the spin. In that way, direct tunneling transitions between the two potential surfaces are favored while keeping the main weight of the wave functions at low energy. We call these oppositely displaced oscillators “antipolaron” states.

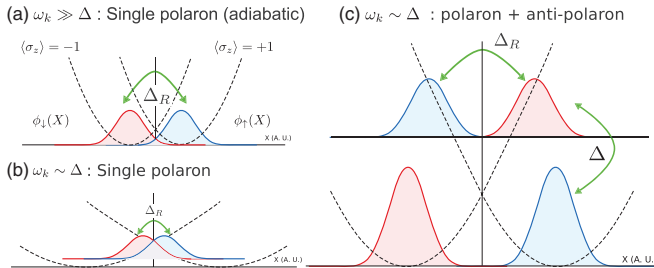


FIG. 1. (Color online) Origins of polaron and antipolaron displacements in environmental wave functions. Black dashed lines are the spin-dependent potential energies of a single harmonic oscillator in the absence of spin tunneling ( $\Delta = 0$ ), while blue (red) curves sketch the single-mode wave functions of the oscillator (in real space  $X$ ) on the  $\langle \sigma_z \rangle = 1(-1)$  potential surfaces. (a) High-frequency modes ( $\omega \gg \Delta$ ) tend to rest in the bottom of their (spin-dependent) potential due to the large energy of other displacements. This leads to the formation of adiabatic polarons. (b) and (c) Low-frequency modes ( $\omega \ll \Delta$ ) have shallow potentials with well-separated minima. The interminima wave-function overlap is reduced while the potential cost of other displacements becomes less prohibitive. The oscillators can either climb up the potential landscape, gaining some tunneling energy [panel (b)], or become superposed with oppositely displaced states—“antipolarons”—so that tunneling and potential energy are both optimal [panel (c)]. Superposition of such polaron and antipolaron states generates multimode entanglement in the complete environmental wave function.

The strong competition between spin tunneling and oscillator displacement cannot indeed be fulfilled by a single coherent state, even if optimized variationally. The latter has been pursued in numerous variational studies [20–24], embodied by the so-called Silbey-Harris (SH) ansatz for the ground state of the spin-boson model [20,21]:

$$|\Psi^{\text{SH}}\rangle = |\uparrow\rangle \otimes |f^{\text{SH}}\rangle - |\downarrow\rangle \otimes |-f^{\text{SH}}\rangle, \quad (2)$$

where the displacements  $f_k^{\text{SH}} = [g_k/2]/(\omega_k + \Delta_R)$  are determined by the variational principle. (Note that this ansatz respects the symmetries of the Hamiltonian in the absence of a magnetic field along  $\hat{z}$ .) While this simple state possesses virtues, such as an accurate estimate of the renormalized tunneling frequency  $\Delta_R = \Delta e^{-2 \sum_k (f_k^{\text{SH}})^2}$ , it also has severe defects, such as spurious transitions [23,25–28] and a drastic underestimation of the qubit coherence  $\langle \sigma_x \rangle$ . Further works aiming at refining the variational ansatz focused on the simple single-mode case [29–31], or were restricted to a non-fully-optimal variational state [32]. In light of the above discussion, the defects of the SH ansatz are readily traced back to the lack of bath entanglement in wave function (2)—only the polaronic response is encoded in  $f_k^{\text{SH}}$ . To capture the missing antipolaronic contributions and so the complete entanglement structure of the bath, we propose here a systematic coherent-state expansion of the many-body ground state:

$$|\Psi\rangle = \sum_{n=1}^N C_n [|\uparrow\rangle \otimes |f^{(n)}\rangle - |\downarrow\rangle \otimes |-f^{(n)}\rangle], \quad (3)$$

with  $|\pm f^{(n)}\rangle = e^{\pm \sum_k f_k^{(n)} (a_k^\dagger - a_k)} |0\rangle$  the  $n$ th coherent state appearing in the wave function. As is well known in many-body and chemical physics, variational methods may be greatly improved with respect to convergence by optimized basis choices. For the spin boson model, coherent states are naturally selected, as was understood from the  $\Delta = 0$  limit, and are in addition very simple to parametrize in terms of displacements. As we will see, the coherent state expansion allows convergence to be achieved with far fewer variational parameters than a brute-force variation of the (exponentially large) coefficients of a full configuration (Fock) basis of the environment states. This is due to the energetic constraints discussed above, which strongly reduce the phase-space volume of the allowed displacements  $f_k^{(n)}$ . Indeed, for  $\omega_k > \Delta_R$ , each displacement function  $f_k^{(n)}$  (for fixed  $n$ ) will undergo quantum fluctuations between the polaronic and antipolaronic branches,  $f_k^{\text{pol}} \simeq g_k / (2\omega_k)$  and  $f_k^{\text{anti}} \simeq -g_k / (2\omega_k)$ , respectively. The main freedom in fixing a given displacement  $f_k^{(n)}$  is then in determining the crossover frequency from polaron to antipolaron behavior. As a consequence (see below), physical properties are very precisely determined for moderate values of  $N$ , the number of coherent states involved in wave function (3).

We can now readily understand how the emergence of environmental entanglement preserves spin coherence at strong dissipation. In the single-polaron Silbey-Harris theory, the spin coherence  $\langle \sigma_x \rangle \simeq e^{-2 \sum_k (f_k^{\text{SH}})^2} = \Delta_R / \Delta$  is incorrectly controlled by the exponentially small renormalized tunneling frequency  $\Delta_R$ . In contrast, the general wave function (3) contains additional contributions to  $\langle \sigma_x \rangle$  of the type  $e^{-\frac{1}{2} \sum_k (f_k^{(n)} + f_k^{(m)})^2}$  for  $n \neq m$ . Quantum fluctuations that favor antipolarons will flip

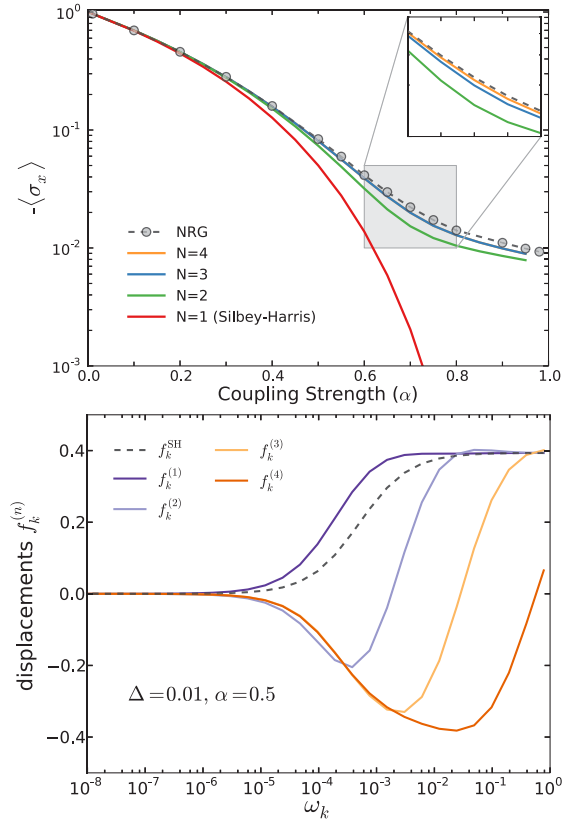


FIG. 2. (Color online) Upper panel: Ground-state coherence  $-\langle\sigma_x\rangle$  as a function of dissipation strength  $\alpha$  computed with the NRG (circles) for  $\Delta/\omega_c = 0.01$  and compared to the results of the expansion Eq. (3) with  $N = 1, 2, 3, 4$  coherent states. The inclusion of an antipolaronic component to the wave function ( $N \geq 2$ ) has a drastic effect on the spin coherence. Lower panel: Displacements determined at order  $N = 1$  (dashed line) and  $N = 4$  (solid lines), showing the emergence of three antipolaron states at low energies, which merge smoothly onto the polaron state at high energy (adiabatic regime) [35]. Parameters are  $\alpha = 0.5$  and  $\Delta/\omega_c = 0.01$ .

the sign of one displacement with respect to the other, reducing the value of the sum, and drastically increasing the exponential with respect to the strongly suppressed value  $\Delta_R/\Delta$ . Thus, environmental correlations built into a multimode Schrödinger cat state affect the qubit properties in a dramatic way.

We now turn to calculating the wave function Eq. (3), where the displacements  $f_k^{(n)}$  and coefficients  $C_n$  are determined by minimizing the total ground-state energy  $E = \langle\Psi|H|\Psi\rangle/\langle\Psi|\Psi\rangle$  for a fixed number  $N$  of coherent states ( $1 \leq n \leq N$ ) [33]. We focus here on the standard case of Ohmic dissipation [6,7], although our results should apply similarly to any type of spectral density. The continuous bath of bosonic excitations then assumes a linear spectrum in frequency,  $J(\omega) \equiv \sum_k g_k^2 \delta(\omega - \omega_k) = 2\alpha\omega\theta(\omega_c - \omega)$ , up to a high-frequency cutoff  $\omega_c$ , while the dissipation strength is given by the dimensionless parameter  $\alpha$ . As a key check on the variational solution, we carry out an exact nonperturbative solution of the SBM using the numerical renormalization group (NRG) [34]; for example, the spin coherence  $\langle\sigma_x\rangle$ , to which we shall compare the variational result, is shown in Fig. 2.

The variational principle leads to a set of displacements  $f_k^{(n)}$ , shown in Fig. 2, that corroborate the physical picture given above: in addition to a fully positive displacement function  $f_k^{(1)}$  (akin to the Silbey-Harris  $f_k^{\text{SH}}$  albeit quantitatively different), we find that all the other displacements undergo a crossover from positive value at high frequency to negative at low frequency. The total wave function (3) is thus strongly entangled.

This environmental entanglement drastically affects the spin coherence  $\langle\sigma_x\rangle$ : note the difference in Fig. 2 between the  $N = 2$  and 1 solutions. In the latter, the coherence is given by the tiny renormalized qubit frequency,  $\Delta_R = \Delta(\Delta e/\omega_c)^{\alpha/(1-\alpha)}$  for  $\Delta/\omega_c \ll 1$ . As the number of polarons increases, however, the variational solution rapidly converges to the exact NRG result, even capturing the saturation at strong dissipation  $-\langle\sigma_x\rangle = \Delta/\omega_c$  for  $\alpha \rightarrow 1$  [36]. These panels thus confirm one important message of our study: emergent entanglement within the environment stabilizes coherence of the spin, a result that is robust with respect to coupling the whole system to a low-temperature thermal bath [33].

We finally provide firm support for the above scenario by developing a many-body quantum tomography technique that allows direct characterization of the ground-state wave function based on nonperturbative NRG computations. While one cannot plot the complete many-body wave function, aspects can be accessed via standard Wigner tomography [1,37], a technique that has witnessed impressive experimental developments lately in the field of superconducting circuits [38–40]. We choose to trace out all modes except the qubit degree of freedom together with a single bath mode with quantum number  $k$ . Projecting first onto only the  $|\uparrow\rangle$  part of the wave function, we obtain the Wigner function  $W_{\uparrow\uparrow}^{(k)}(X)$  as a function of the displacement  $X$  of oscillator  $k$ . For the wave function (3), this has a straightforward interpretation [1,33]: the probability in phase space is simply the sum of Gaussian peaks centered at  $X \simeq (f_k^{(n)} + f_k^{(m)})/2$ . For high-energy modes (adiabatic regime), all displacements are polaronic,  $f_k^{(n)} \simeq f_k^{\text{cl}} = g_k/(2\omega_k)$ , so that a single shifted Gaussian appears in  $W_{\uparrow\uparrow}^{(k)}(X)$ ; see Fig. 3(a). A single coherent state [i.e., the ansatz (2)] is sufficient in this high-frequency regime to reproduce the NRG data perfectly, demonstrating the presence of polarons in the wave function.

Antipolarons appear more clearly in the spin off-diagonal ground-state Wigner function  $W_{\uparrow\downarrow}^{(k)}(X)$ , rather than in  $W_{\uparrow\uparrow}^{(k)}(X)$ . Note that such conditional Wigner tomography was considered, for instance, in recent measurements of the moments  $\langle(a^\dagger)^n (a)^m \sigma^i\rangle$  for a carefully prepared state entangling microwave photons and a superconducting qubit in a circuit QED experiment [40]. In  $W_{\uparrow\downarrow}^{(k)}(X)$ , the antipolarons are hidden because their weights  $C_n$  tend to be smaller than that of the main polaron. In contrast,  $W_{\uparrow\downarrow}^{(k)}(X)$  is governed by cross polaron-antipolaron contributions which peak at  $X \simeq \pm(f_k^{(n)} - f_k^{(m)})/2$  [33]; other terms of polaron-polaron type have an exponentially small weight of order  $\Delta_R$ . The emergence of antipolaronic, namely opposite, displacements in  $f_k^{(n)}$  and  $f_k^{(m)}$  should thus appear as a pair of symmetric Gaussians in  $W_{\uparrow\downarrow}^{(k)}(X)$ . This is indeed observed in the NRG data for intermediate frequencies, when adiabatic and antiadiabatic

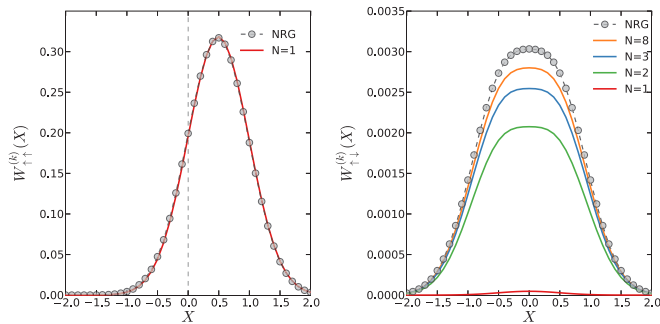


FIG. 3. (Color online) Left: Spin-diagonal Wigner distribution, as obtained from the NRG, computed for a high-energy mode. Polaron formation leads to a classical shift,  $X = f_k^{\text{cl}}$ , that is fully captured by the Silbey-Harris state (single coherent state). Right: The spin-off-diagonal Wigner function is badly approximated by the single polaron  $N = 1$  state, as antipolaron contributions dominate in this quantity. A single antipolaron ( $N = 2$ ) quickly restores the correct magnitude, and reveals a pair of shifted Gaussians, as expected (see text). (Parameters here are  $\alpha = 0.8$  and  $\Delta/\omega_c = 0.01$ .)

entanglement is maximal, as shown in Fig. 3(b). In this case, a single coherent state (fully polaronic) completely fails, but our expansion (3) quickly converges to the NRG results.

In conclusion, we have shown how environmental entanglement emerges in the ground-state wave function of the spin-boson model, and why it surprisingly has a dramatic influence on the qubit coherence. This understanding led us to develop a general framework to rationalize many-body wave functions in strongly interacting open quantum systems. Proposals have been made to realize the strongly dissipative spin-boson model in various physical systems [42,43], most notably by coupling a superconducting qubit to Josephson junction arrays [41,44], giving hope that experimental studies of environmental states should become accessible in the near future. The advances made in the present work open the door to a better understanding of several interesting issues, such as photon transport in dissipative models [41,44], quantum phase transitions for sub-Ohmic baths [16,34], and studies of biased spin-boson systems [23].

S.B., S.F., and H.U.B. thank the Grenoble Nanoscience Foundation for funding under RTRA Contract CORTRANO, and support by the US DOE, Division of Materials Sciences and Engineering, under Grant No. DE-SC0005237, is gratefully acknowledged. A.N. thanks Imperial College and the University of Manchester for support. A.W.C. acknowledges support from the Winton Programme for the Physics of Sustainability.

- [1] J. M. Raimond and S. Haroche, *Exploring the Quantum*, Oxford Graduate Series (Oxford University Press, Oxford, 2006).
- [2] A. M. Nielsen and I. L. Chuang, *Quantum Computation and Quantum Information* (Cambridge University Press, New York, 2007).
- [3] A. Nitzan, *Chemical Dynamics in Condensed Phases: Relaxation, Transfer and Reactions in Condensed Molecular Systems* (Oxford University Press, Oxford, 2006).
- [4] N. Lambert, Y.-N. Chen, Y.-C. Cheng, C.-J. Li, G.-Y. Chen, and F. Nori, *Nat. Phys.* **9**, 10 (2013).
- [5] A. W. Chin, J. Prior, R. Rosenbach, F. Caycedo-Soler, S. F. Huelga, and M. B. Plenio, *Nat. Phys.* **9**, 113 (2013).
- [6] A. J. Leggett, S. Chakravarty, A. T. Dorsey, M. P. A. Fisher, A. Garg, and W. Zwerger, *Rev. Mod. Phys.* **59**, 1 (1987).
- [7] U. Weiss, *Quantum Dissipative Systems* (World Scientific, Singapore, 1993).
- [8] H.-P. Breuer and F. Petruccione, *The Theory of Open Quantum Systems* (Oxford University Press, Oxford, 2010).
- [9] G. Scholes, G. Fleming, A. Olaya-Castro, and R. van Grondelle, *Nat. Chem.* **3**, 763 (2011).
- [10] D. Jennings, A. Dragan, S. D. Barrett, S. D. Bartlett, and T. Rudolph, *Phys. Rev. A* **80**, 032328 (2009).
- [11] R. Raussendorf and H. J. Briegel, *Phys. Rev. Lett.* **86**, 5188 (2001).
- [12] R. Bulla, T. A. Costi, and T. Pruschke, *Rev. Mod. Phys.* **80**, 395 (2008).
- [13] N. Makri, *J. Math. Phys.* **36**, 2430 (1995).
- [14] H. Wang and M. Thoss, *New J. Phys.* **10**, 115005 (2008).
- [15] P. Nalbach and M. Thorwart, *Phys. Rev. B* **81**, 054308 (2010).
- [16] A. Winter, H. Rieger, M. Vojta, and R. Bulla, *Phys. Rev. Lett.* **102**, 030601 (2009).
- [17] A. Alvermann and H. Fehske, *Phys. Rev. Lett.* **102**, 150601 (2009).
- [18] J. Prior, A. W. Chin, S. F. Huelga, and M. B. Plenio, *Phys. Rev. Lett.* **105**, 050404 (2010).
- [19] S. Florens, A. Freyn, D. Venturelli, and R. Narayanan, *Phys. Rev. B* **84**, 155110 (2011).
- [20] V. J. Emery and A. Luther, *Phys. Rev. Lett.* **26**, 1547 (1971).
- [21] R. Silbey and R. A. Harris, *J. Chem. Phys.* **80**, 2615 (1984); R. A. Harris and R. Silbey, *ibid.* **83**, 1069 (1985).
- [22] A. W. Chin, J. Prior, S. F. Huelga, and M. B. Plenio, *Phys. Rev. Lett.* **107**, 160601 (2011).
- [23] A. Nazir, D. P. S. McCutcheon, and A. W. Chin, *Phys. Rev. B* **85**, 224301 (2012).
- [24] K. Agarwal, I. Martin, M. D. Lukin, and E. Demler, *Phys. Rev. B* **87**, 144201 (2013).
- [25] D. P. S. McCutcheon and A. Nazir, *J. Chem. Phys.* **135**, 114501 (2011).
- [26] C. K. Lee, J. Moix, and J. Cao, *J. Chem. Phys.* **136**, 204120 (2012).
- [27] A. Chin and M. Turlakov, *Phys. Rev. B* **73**, 075311 (2006).
- [28] Z.-D. Chen and H. Wong, *Phys. Rev. B* **78**, 064308 (2008).
- [29] J. Stolze and L. Müller, *Phys. Rev. B* **42**, 6704 (1990).
- [30] Q.-B. Ren and Q.-H. Chen, *Chin. Phys. Lett.* **22**, 2914 (2005).
- [31] M.-J. Hwang and M.-S. Choi, *Phys. Rev. A* **82**, 025802 (2010).
- [32] H. Zheng and Z. Lü, *J. Chem. Phys.* **138**, 174117 (2013).
- [33] See Supplemental Material at <http://link.aps.org/supplemental/10.1103/PhysRevB.89.121108> for details on the coherent states expansion, on the NRG calculations, and on finite temperature effects.
- [34] R. Bulla, N.-H. Tong, and M. Vojta, *Phys. Rev. Lett.* **91**, 170601 (2003).

- [35] In the NRG logarithmic discretization of the bath spectrum, frequency points are unevenly spaced, leading to a saturation of  $f_k$  at high frequencies instead of the falloff obtained for a linear energy mesh.
- [36] K. Le Hur, *Ann. Phys. (N.Y.)* **323**, 2208 (2008).
- [37] A. I. Lvovsky and M. G. Raymer, *Rev. Mod. Phys.* **81**, 299 (2009).
- [38] M. Hofheinz, H. Wang, M. Ansmann, R. C. Bialczak, E. Lucero, M. Neeley, A. D. O'Connell, D. Sank, J. Wenner, J. M. Martinis, and A. N. Cleland, *Nature (London)* **459**, 546 (2009).
- [39] C. Eichler, D. Bozyigit, C. Lang, L. Steffen, J. Fink, and A. Wallraff, *Phys. Rev. Lett.* **106**, 220503 (2011).
- [40] C. Eichler, C. Lang, J. M. Fink, J. Govenius, S. Filipp, and A. Wallraff, *Phys. Rev. Lett.* **109**, 240501 (2012).
- [41] K. Le Hur, *Phys. Rev. B* **85**, 140506 (2012).
- [42] A. Recati, P. O. Fedichev, W. Zwerger, J. von Delft, and P. Zoller, *Phys. Rev. Lett.* **94**, 040404 (2005).
- [43] D. Porras, F. Marquardt, J. von Delft, and J. I. Cirac, *Phys. Rev. A* **78**, 010101(R) (2008).
- [44] M. Goldstein, M. H. Devoret, M. Houzet, and L. I. Glazman, *Phys. Rev. Lett.* **110**, 017002 (2013).